

## Atomic-scale characterization of germanium isotopic multilayers by atom probe tomography

Y. Shimizu, H. Takamizawa, Y. Kawamura, M. Uematsu, T. Toyama et al.

Citation: *J. Appl. Phys.* **113**, 026101 (2013); doi: 10.1063/1.4773675

View online: <http://dx.doi.org/10.1063/1.4773675>

View Table of Contents: <http://jap.aip.org/resource/1/JAPIAU/v113/i2>

Published by the [American Institute of Physics](#).

---

### Related Articles

Defect engineering of the oxygen-vacancy clusters formation in electron irradiated silicon by isovalent doping: An infrared perspective

*J. Appl. Phys.* **112**, 123517 (2012)

Band bending and determination of band offsets in amorphous/crystalline silicon heterostructures from planar conductance measurements

*J. Appl. Phys.* **112**, 123717 (2012)

A transition of three to two dimensional Si growth on Ge (100) substrate

*J. Appl. Phys.* **112**, 126101 (2012)

Fabrication of large-grained thin polycrystalline silicon films on foreign substrates by titanium-assisted metal-induced layer exchange

*J. Appl. Phys.* **112**, 123509 (2012)

Effect of silicon/crucible interfacial energy on orientation of multicrystalline silicon ingot in unidirectional growth

*J. Appl. Phys.* **112**, 113521 (2012)

---

### Additional information on *J. Appl. Phys.*

Journal Homepage: <http://jap.aip.org/>

Journal Information: [http://jap.aip.org/about/about\\_the\\_journal](http://jap.aip.org/about/about_the_journal)

Top downloads: [http://jap.aip.org/features/most\\_downloaded](http://jap.aip.org/features/most_downloaded)

Information for Authors: <http://jap.aip.org/authors>

## ADVERTISEMENT



**AIP Advances**

Now Indexed in Thomson Reuters Databases

Explore AIP's open access journal:

- Rapid publication
- Article-level metrics
- Post-publication rating and commenting

## Atomic-scale characterization of germanium isotopic multilayers by atom probe tomography

Y. Shimizu,<sup>1,a)</sup> H. Takamizawa,<sup>1</sup> Y. Kawamura,<sup>2</sup> M. Uematsu,<sup>2</sup> T. Toyama,<sup>1</sup> K. Inoue,<sup>1</sup> E. E. Haller,<sup>3</sup> K. M. Itoh,<sup>2</sup> and Y. Nagai<sup>1</sup>

<sup>1</sup>The Oarai Center, Institute for Materials Research, Tohoku University, 2145-2 Narita, Oarai, Ibaraki 311-1313, Japan

<sup>2</sup>School of Fundamental Science and Technology, Keio University, 3-14-1 Hiyoshi, Kohoku-ku, Yokohama 223-8522, Japan

<sup>3</sup>University of California at Berkeley and Lawrence Berkeley National Laboratory, 1 Cyclotron Road, Berkeley, California 94720, USA

(Received 25 November 2012; accepted 11 December 2012; published online 8 January 2013)

We report comparison of the interfacial sharpness characterization of germanium (Ge) isotopic multilayers between laser-assisted atom probe tomography (APT) and secondary ion mass spectrometry (SIMS). An alternating stack of 8-nm-thick naturally available Ge layers and 8-nm-thick isotopically enriched <sup>70</sup>Ge layers was prepared on a Ge(100) substrate by molecular beam epitaxy. The APT mass spectra consist of clearly resolved peaks of five stable Ge isotopes (<sup>70</sup>Ge, <sup>72</sup>Ge, <sup>73</sup>Ge, <sup>74</sup>Ge, and <sup>76</sup>Ge). The degree of intermixing at the interfaces between adjacent layers was determined by APT to be around  $0.8 \pm 0.1$  nm which was much sharper than that obtained by SIMS. © 2013 American Institute of Physics. [<http://dx.doi.org/10.1063/1.4773675>]

Technological interest in germanium (Ge) as an electronic material is increasing, thanks to its higher carrier mobilities than those found in silicon (Si).<sup>1</sup> Among many device processing related issues, an in-depth understanding of the dopant diffusion and electrical activation in Ge is crucial for the realization of Ge-based integrated circuits. Isotopic multilayer Ge samples are ideal for experimental probing of dopant behavior during impurity doping (e.g., ion implantation) and subsequent thermal cycles for activation, since they enable us to evaluate not only the behavior of the dopant but also that of host Ge atoms simultaneously.<sup>2-8</sup>

The isotopic multilayers which we studied are composed typically of alternating layers of different stable isotopes and have been shown useful for the investigation of self-migration by probing the change in the spatial distribution of various isotopes around the interfaces.<sup>2-8</sup> Such isotopic multilayers are fabricated by molecular beam epitaxy and/or chemical vapor deposition using isotopically-enriched sources to control the stable isotopic composition along the growth direction. Diffusion of dopants and host semiconductor atoms can be probed simultaneously by probing the dopant depth profiles and the sharpness of isotopic interfaces by secondary ion mass spectrometry (SIMS). However, the artifacts caused mainly by a primary ion bombardment, i.e., atomic mixing, during the SIMS measurement are detrimental especially when atomic-scale evaluation of dopant and host-atom migration are needed for state-of-the-art device development. The spatial resolution of SIMS, as we will show in this work for Ge, is far insufficient for atomic-scale characterization. Moreover, SIMS profiling is limited to one-dimension. Therefore, a method to probe distribution of dopants and host semiconductor atoms in three-dimension with the spatial resolution of the atomic level is needed. In this

regard, the laser-assisted atom probe tomography (APT) is an excellent candidate.

Laser-assisted APT has been adopted originally for practical metrology<sup>9-12</sup> and employed subsequently for three-dimensional (3D) elemental mapping of modern electronic device structures<sup>13-16</sup> and quantitative evaluation of the interface sharpness of layer structures<sup>17-25</sup> with the order of atomic-scale resolution. The unsurpassed spatial and isotopic resolutions of APT have been proven already in characterization of <sup>28</sup>Si/<sup>30</sup>Si interfaces in Si isotopic heterostructures.<sup>17-19</sup> The present paper demonstrates atomic-scale characterization of Ge isotopic multilayers composed of a stack of isotopically-enriched <sup>70</sup>Ge and naturally available Ge (referred to as <sup>nat</sup>Ge hereafter) layers. Note that <sup>nat</sup>Ge is composed of five stable isotopes in the fixed composition (<sup>70</sup>Ge: 20.5%, <sup>72</sup>Ge: 27.4%, <sup>73</sup>Ge: 7.8%, <sup>74</sup>Ge: 36.5%, and <sup>76</sup>Ge: 7.8%).<sup>26</sup>

The structure of the Ge isotopic multilayers employed in this work is shown in Fig. 1(a) and detailed descriptions of such sample preparation are given in Refs. 6 and 7. In short, a 2-in. (100) <sup>nat</sup>Ge wafer was employed as a substrate. A ~100 nm-thick <sup>nat</sup>Ge buffer layer was grown to form a smooth surface followed by the growth of periodic layers of isotopically-enriched <sup>70</sup>Ge and <sup>nat</sup>Ge at a substrate temperature of 250 °C. The isotopic multilayers were composed of five stacks of enriched <sup>70</sup>Ge(8 nm)/<sup>nat</sup>Ge(8 nm) pair layers with a ~50 nm-thick <sup>nat</sup>Ge cap layer on the top. The <sup>nat</sup>Ge capping works as a protection layer against the <sup>69</sup>Ga focused ion beam (FIB) irradiation used to shape the structure into a needle as outlined in Fig. 1(a). A laser-assisted local-electrode atom probe (LEAP3000X HR, Ametek) with a green laser (wavelength: 532 nm) was employed for APT. The pulsed laser power was 0.5 nJ with a frequency of 200 kHz. The ion detection efficiency was approximately 37%. The base temperature of the needle specimens was cooled down to 50 K to inhibit surface migration during

<sup>a)</sup>Electronic mail: yshimizu@imr.tohoku.ac.jp.

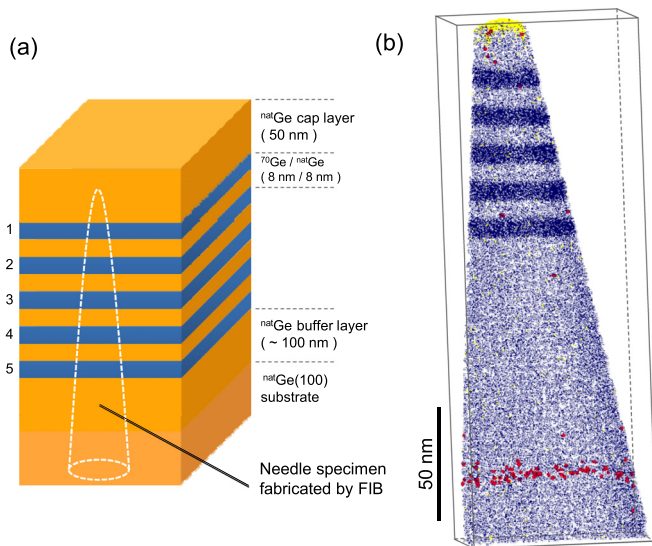


FIG. 1. (a) A schematic illustration of the Ge isotopic multilayers. The outline of the needle specimen for APT is also shown. (b) A 3D reconstructed mapping (20 nm-slice) of  $^{70}\text{Ge}$  (dark blue),  $^{69}\text{Ga}$  (yellow), and  $^{12}\text{C}$  (red) atoms in a volume of  $80 \times 80 \times 230 \text{ nm}^3$ . Only 5% of the entire atoms are displayed for the  $^{70}\text{Ge}$  mapping.

ionization and extraction of the atoms from the needle. For the 3D mapping of the Ge isotopes using the Integrated Visualization and Analysis Software (IVAS) protocol,<sup>27</sup> singly ( $\text{Ge}^+$ ) and doubly charged ( $\text{Ge}^{2+}$ ) peaks were selected. The charge state ratio,  $\text{Ge}^{2+}/\text{Ge}^+$ , was approximately 0.17. For comparison with respect to the depth resolution, SIMS measurements (PHI ADEPT1010) were performed to obtain the depth profiles of  $^{70}\text{Ge}$  and  $^{74}\text{Ge}$ .

Figure 1(b) exhibits a 3D mapping image of the  $^{70}\text{Ge}$  composition in the Ge isotopic multilayer samples. In this map,  $^{69}\text{Ga}$  was seen in the  $^{\text{nat}}\text{Ge}$  capping layer only, indicating that the stacks of  $^{70}\text{Ge}/^{\text{nat}}\text{Ge}$  layers were not damaged during sample preparation by the Ga FIB. In addition, a pile-up of residual  $^{12}\text{C}$  atoms was observed at the interface between the  $^{\text{nat}}\text{Ge}$  buffer layer and the  $^{\text{nat}}\text{Ge}$  substrate. In fact, we use this carbon pile-up to identify the position of the substrate surface in the APT analysis. It should also be noted that the planar interfaces guaranteed for the  $^{70}\text{Ge}/^{\text{nat}}\text{Ge}$  sample prepared by the layer-by-layer growth can serve as the guideline for improving the 3D image reconstruction presenting the IVAS protocol.

Figure 2(a) shows the atom mapping for the all five stable Ge isotopes ( $^{70}\text{Ge}$ ,  $^{72}\text{Ge}$ ,  $^{73}\text{Ge}$ ,  $^{74}\text{Ge}$ , and  $^{76}\text{Ge}$ ) in the Ge isotopic multilayers. The mass spectra of  $\text{Ge}^+$  and  $\text{Ge}^{2+}$  signals obtained from the first  $^{70}\text{Ge}$  and  $^{\text{nat}}\text{Ge}$  pair are shown in Figs. 2(b) and 2(c), respectively. From the integrated areas of the  $\text{Ge}^+$  and  $\text{Ge}^{2+}$  peaks, we can deduce the isotopic composition in the enriched  $^{70}\text{Ge}$  solid-source (Fig. 2(b)):  $^{70}\text{Ge}$ :  $95.78\% \pm 0.64\%$ ,  $^{72}\text{Ge}$ :  $4.15\% \pm 0.13\%$ ,  $^{73}\text{Ge}$ :  $0.03\% \pm 0.01\%$ ,  $^{74}\text{Ge}$ :  $0.03\% \pm 0.01\%$ , and  $^{76}\text{Ge}$ :  $0.01\% \pm 0.01\%$ . The isotopic composition in the  $^{\text{nat}}\text{Ge}$  layer (Fig. 2(c)) is also obtained in the same manner:  $^{70}\text{Ge}$ :  $20.68\% \pm 0.32\%$ ,  $^{72}\text{Ge}$ :  $28.02\% \pm 0.37\%$ ,  $^{73}\text{Ge}$ :  $7.88\% \pm 0.20\%$ ,  $^{74}\text{Ge}$ :  $36.21\% \pm 0.42\%$ , and  $^{76}\text{Ge}$ :  $7.22\% \pm 0.19\%$ , which is in good agreement with the established values of natural isotopic abundances.<sup>26</sup>

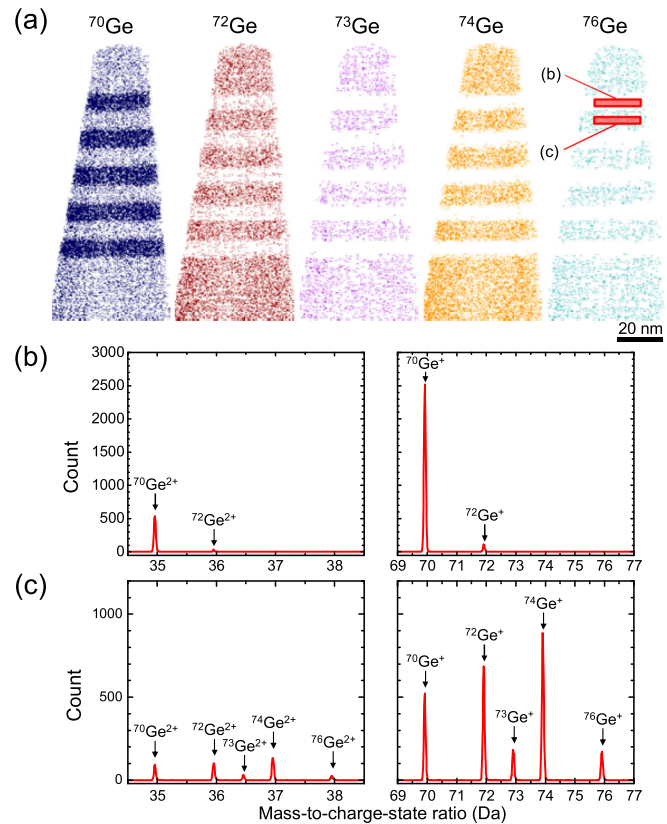


FIG. 2. (a) The atom mapping of the five Ge stable isotopes ( $^{70}\text{Ge}$ ,  $^{72}\text{Ge}$ ,  $^{73}\text{Ge}$ ,  $^{74}\text{Ge}$ , and  $^{76}\text{Ge}$ ) in the Ge isotopic multilayers. Doubly ( $\text{Ge}^{2+}$ ) and singly charged ( $\text{Ge}^+$ ) peaks in the mass spectra in the 1st pair of the  $^{70}\text{Ge}$  and  $^{\text{nat}}\text{Ge}$  layers (selected volume:  $20 \times 20 \times 3 \text{ nm}^3$ ) are shown in (b) and (c), respectively.

Figure 3(a) shows the depth profiles of the  $^{70}\text{Ge}$  and  $^{74}\text{Ge}$  (the most abundant stable isotope in  $^{\text{nat}}\text{Ge}$ ) obtained from the integration within the cross-sectional area of  $10 \times 10 \text{ nm}^2$ , together with the profiles by SIMS under the bombardment of primary ions  $\text{Cs}^+$  with an energy of 1 keV. Apparently, the APT profiles show much sharper interfaces than the ones recorded by SIMS. Although the SIMS profiles do not show the plateau regions in both the enriched  $^{70}\text{Ge}$  and  $^{\text{nat}}\text{Ge}$  layers, APT profiles exhibit steeper interfaces, thanks to the absence of artifacts such as atomic mixing. Enlarged mapping of the five stacks of  $^{70}\text{Ge}/^{\text{nat}}\text{Ge}$  layers in a volume of  $10 \times 10 \times 100 \text{ nm}^3$  is displayed in Fig. 3(b) for both  $^{70}\text{Ge}$  and  $^{74}\text{Ge}$ . For highlighting the  $^{70}\text{Ge}/^{\text{nat}}\text{Ge}$  interfaces, the iso-concentration surface of 50% of  $^{70}\text{Ge}$  is shown in both of the  $^{70}\text{Ge}$  and  $^{74}\text{Ge}$  mappings. In this analysis, the averaged surface roughness ( $S_d$ : the average of the absolute values of the measured height deviations from the ideally flat interface) for ten iso-concentration surfaces was found to be  $0.10 \pm 0.01 \text{ nm}$  in the area of  $10 \times 10 \text{ nm}^2$ .

Let us now discuss the comparison of the present results on Ge with those obtained for Si previously. For Si, APT analysis has been proven useful for obtaining dopant distribution and interface structures in modern electronic device structures.<sup>13–16</sup> Our recent APT characterization of Si isotopic multilayers showed very high spatial resolution, 0.4 nm/decade, at interfaces of  $^{28}\text{Si}/^{30}\text{Si}$  heterostructures.<sup>18</sup> In order to evaluate the interfacial sharpness at each specific

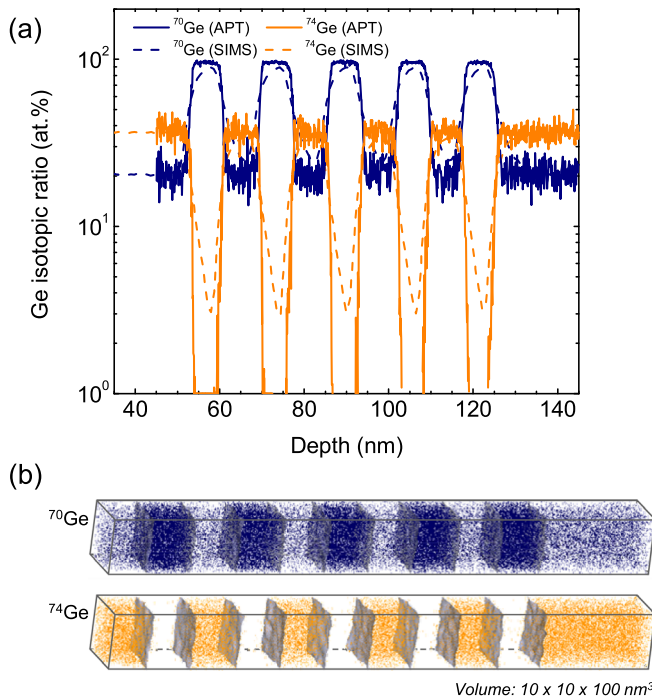


FIG. 3. (a) Depth profiles by APT (solid curves) of  $^{70}\text{Ge}$  and  $^{74}\text{Ge}$  in the Ge isotopic multilayers obtained from an area of  $10 \times 10 \text{ nm}^2$ , overlaid with the SIMS profiles (broken curves). (b)  $^{70}\text{Ge}$  and  $^{74}\text{Ge}$  mappings in a volume of  $10 \times 10 \times 100 \text{ nm}^3$  with the iso-concentration surfaces of  $^{70}\text{Ge}$  at 50% for highlighting the  $^{70}\text{Ge}/^{\text{nat}}\text{Ge}$  interfaces.

interface, the proximity histogram composition<sup>28</sup> (proxigram: a profile of local atomic concentrations vs. proximity to an interface) is employed for this assessment. Figure 4 shows the proxigram of  $^{70}\text{Ge}$  across the  $^{70}\text{Ge}/^{\text{nat}}\text{Ge}$  within an area of  $10 \times 10 \text{ nm}^2$ , overlaid with  $^{28}\text{Si}$  profile at  $^{28}\text{Si}/^{30}\text{Si}$  interface. Both the Ge and Si samples were measured under practically the same conditions (APT apparatus: LEAP3000X HR, laser wavelength: 532 nm, sample base temperature: 50 K, laser power: 0.5 nJ). The slope at the  $^{70}\text{Ge}/^{\text{nat}}\text{Ge}$  interface was determined to be  $0.8 \pm 0.1 \text{ nm}$  by evaluating the 16%–84% concentration change<sup>29</sup> in the  $^{70}\text{Ge}$  profile. Figure 4 shows very little difference in the

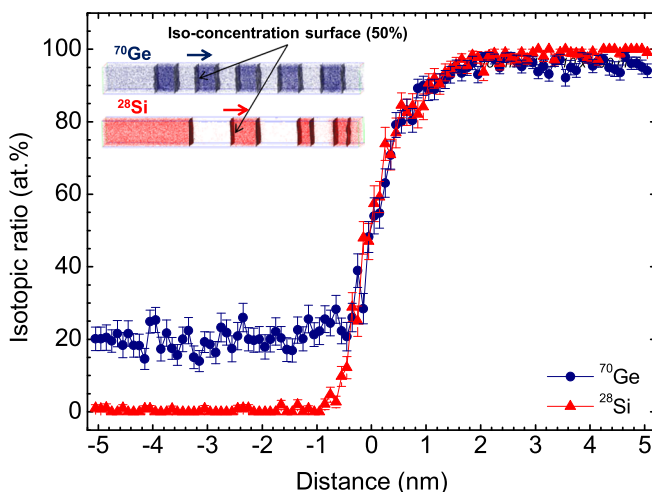


FIG. 4. Proximity histogram composition profiles of  $^{70}\text{Ge}$  and  $^{28}\text{Si}$  isotopes across the iso-concentration surface of 50% for Ge and Si isotopic multilayers, respectively.

sharpness of the Ge and Si samples measured by APT. However, the evaporation field required for Ge is lower than that for Si ( $\text{Ge}^{2+}$ : 29 V/nm,  $\text{Si}^{2+}$ : 33 V/nm).<sup>30</sup> Due to the lower electric field required for Ge, one can evaporate an atom on needle apex with lower standing voltage than in Si, which allows suppression of sample fracture probability during APT measurements. This advantage is of importance for characterizing advanced Ge-based electronic devices with high yield ratio.

In summary, the isotopic concentration profiles in  $^{70}\text{Ge}/^{\text{nat}}\text{Ge}$  multilayer samples were obtained by laser-assisted atom probe tomography. The 3D atomic distributions of the five Ge stable isotopes were clearly resolved using singly and doubly charged Ge peaks in the atom probe tomography mass spectra. The sharpness of the interface  $0.8 \pm 0.1 \text{ nm}$  revealed by the atom probe was much steeper than the depth profiles obtained by SIMS. The intrinsic spatial resolution obtained for germanium is approximately the same with the one obtained for silicon in the past.

Y.S. wishes to thank Dr. M. Tomita of Toshiba Corporation for fruitful discussions. The work at Tohoku University was supported in part by Grants-in-Aid for Scientific Research from MEXT (Grants Nos. 21246142 and 24760246) and STARC. The work at Keio University has been supported in part by the Grant-in-Aid for Scientific Research and Project for Developing Innovation Systems by MEXT, FIRST, and CREST–JST. The work at LBNL was supported in part by the U.S. Department of Energy, Office of Basic Energy Sciences, Materials Sciences and Engineering Division, under Contract No. DE-AC02-05CH11231.

<sup>1</sup>C. Claeys and E. Simoen, *Germanium-Based Technologies—From Materials to Devices* (Elsevier, Amsterdam, 2007).

<sup>2</sup>H. Bracht *et al.*, *Phys. Rev. B* **75**, 035211 (2007).

<sup>3</sup>Y. Shimizu *et al.*, *J. Appl. Phys.* **105**, 013504 (2009).

<sup>4</sup>Y. Shimizu *et al.*, *Appl. Phys. Express* **1**, 021401 (2008).

<sup>5</sup>S. Brotzmann *et al.*, *Phys. Rev. B* **77**, 235207 (2008).

<sup>6</sup>M. Naganawa *et al.*, *Appl. Phys. Lett.* **93**, 191905 (2008).

<sup>7</sup>Y. Kawamura *et al.*, *Appl. Phys. Express* **3**, 071303 (2010).

<sup>8</sup>H. Bracht *et al.*, *J. Appl. Phys.* **110**, 093502 (2011).

<sup>9</sup>T. F. Kelly and D. J. Larson, *Mater. Charact.* **44**, 59 (2000).

<sup>10</sup>B. Gault *et al.*, *Rev. Sci. Instrum.* **77**, 043705 (2006).

<sup>11</sup>T. F. Kelly and M. K. Miller, *Rev. Sci. Instrum.* **78**, 031101 (2007).

<sup>12</sup>K. Hono *et al.*, *Ultramicroscopy* **111**, 576 (2011).

<sup>13</sup>D. J. Larson *et al.*, *J. Phys.: Conf. Ser.* **326**, 012030 (2011).

<sup>14</sup>H. Takamizawa *et al.*, *Appl. Phys. Lett.* **99**, 133502 (2011).

<sup>15</sup>A. K. Kambham *et al.*, *Ultramicroscopy* **111**, 535 (2011).

<sup>16</sup>H. Takamizawa *et al.*, *Appl. Phys. Lett.* **100**, 093502 (2012).

<sup>17</sup>Y. Shimizu *et al.*, *J. Appl. Phys.* **106**, 076102 (2009).

<sup>18</sup>Y. Shimizu *et al.*, *J. Appl. Phys.* **109**, 036102 (2011).

<sup>19</sup>O. Moutanabbir *et al.*, *Appl. Phys. Lett.* **98**, 013111 (2011).

<sup>20</sup>S. Koelling *et al.*, *Appl. Phys. Lett.* **95**, 144106 (2009).

<sup>21</sup>E. Cadel *et al.*, *J. Appl. Phys.* **106**, 044908 (2009).

<sup>22</sup>D. E. Perea *et al.*, *Nat. Nanotechnol.* **4**, 315 (2009).

<sup>23</sup>Z. Balogh *et al.*, *Appl. Phys. Lett.* **99**, 181902 (2011).

<sup>24</sup>M. Müller *et al.*, *Appl. Phys. Lett.* **100**, 083109 (2012).

<sup>25</sup>Y. Ashuach *et al.*, *Appl. Phys. Lett.* **100**, 241604 (2012).

<sup>26</sup>E. E. Haller, *J. Appl. Phys.* **77**, 2857 (1995).

<sup>27</sup>B. Gault *et al.*, *Ultramicroscopy* **111**, 448 (2011).

<sup>28</sup>O. C. Hellman *et al.*, *Microsc. Microanal.* **6**, 437 (2000).

<sup>29</sup>ASTM Standard Terminology Relating to Surface Analysis, E 673-91c American Society for Testing and Materials, Committee E-42 on Surface Analysis, Philadelphia, PA, 1992.

<sup>30</sup>M. K. Miller, *Atom Probe Tomography: Analysis at the Atomic Level* (Springer, New York, 2000).